High temperature Bose-Einstein condensation into an excited state at equilibrium

Raina J. Olsen*
Materials Science and Technology Division, Oak Ridge National Laboratory, Oak Ridge, TN 37831, USA

We describe Bose-Einstein condensation of strongly interacting particles into a quantum state which is an excited single-particle state, but becomes the many-body ground state as density increases because it minimizes the interaction energy compared to other states. Mean field calculations for a graphene potential just wide enough for two closely interacting layers of molecular hydrogen show condensation at temperatures up to 60 K. In the condensed state, molecules hop between layers, increasing the first peak in the pair-correlation function just past the hard core repulsion diameter.

PACS numbers: 67.85.Hj, 67.85.Jk, 05.30.-d, 67.63.Cd

A Bose-Einstein condensate (BEC) is a delicate state of ultra-cold matter in which a significant fraction of boson particles occupy the single lowest energy quantum state. While condensation was long suspected to play a role in superfluid helium [1], the existance of a BEC was experimentally demonstrated [2–4] only recently. Since then, the primary application of the phenomenon has been in providing a macroscopic quantum object consisting of many particles acting in perfect unison, which can be probed in search of first principles for quantum mechanics. A BEC only forms when the density of available quantum states (DOS) is reduced to the order of the actual density, requiring temperatures $T \leq 2.2$ Kelvin (K).

In this letter, we describe a new breed of BEC which forms from strongly interacting bosons that condense into a state with non-zero kinetic energy. The state minimizes the interaction energy, creating an energetic preference for the condensate which is able to overcome the entropic cost of multiple occupation at higher temperatures than a traditional BEC. We show calculations using mean field theory for molecular hydrogen (H_2) confined in a graphene potential with a precisely tuned width in which H_2 forms two closely interacting layers. For an excited state in which a molecule hops between layers (Fig 1(c)), the first peak in the pair-correlation function [5] for two condensed H_2 is increased past the hard core repulsion diameter [6], reducing their interaction relative to any other pair of occupied states and producing a condensate at temperatures up to 60 K.

These relatively high temperatures will allow experimental studies under conditions which are considerably less delicate than those currently required. In addition, to our knowledge this is the first system for which bosons can be shown to condense into an excited state at equilibrium, without being driven by external conditions, as occurs with lasers [7], condensates of quasi-particle excitations [8, 9], and vortices [10–12], solitons [13, 14], and phonon-like collective oscillations[15] evoked in typical BECs. As such, this condensate may provide a venue for new discoveries about quantum mechanics.

Hydrogen adsorption potentials created by two parallel graphene layers[16] with AA stacking separated by

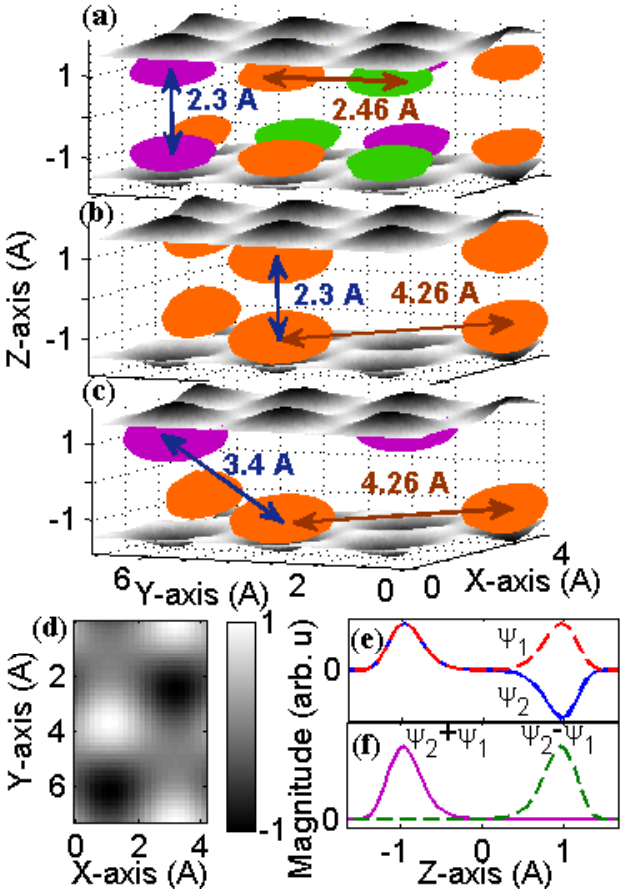

FIG. 1. Quantum states of H_2 in a 8.1 Å wide graphene slit-pore. The V=0 potential energy surfaces enclosing the adsorption volume are shown. Shaded ovals show regions of most concentrated probability density for three states: (a) a thermally averaged state at T =20 K (Color differences aid in distinguishing peaks.) (b) an aligned commensurate (AC) state (c) a staggered commensurate (SC) state. Remaining panels depict formation of SC state in Eq. 3. (d) A wavefunction at the Dirac point. The magnitude at each hexagon center of the graphene is alteratively +1, 0, and -1. Alternation between the top and bottom occurs by combination of (e) the first two vibrational wavefunctions. (f) Adding/subtracting them concentrates the wavefunction at the top/bottom.

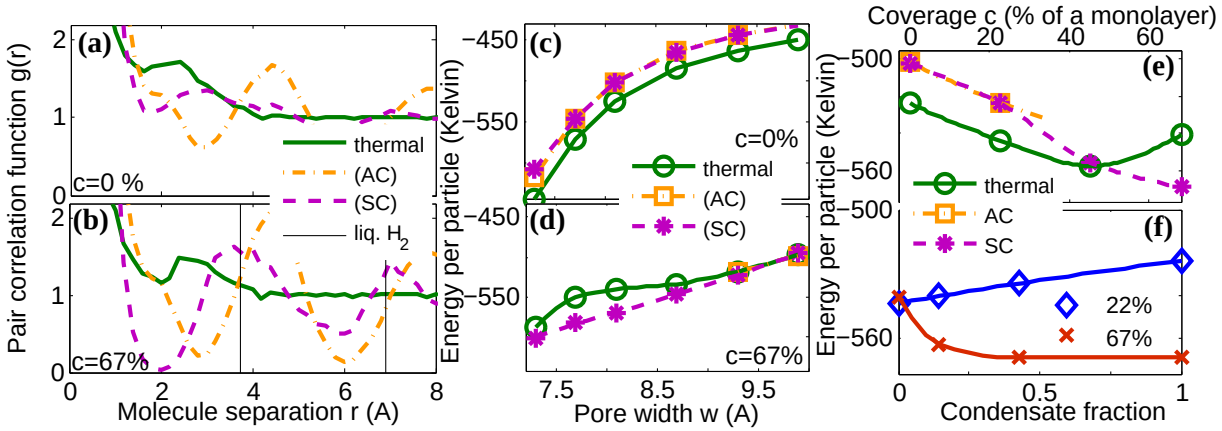

FIG. 2. Properties of H_2 in a thermal distribution of states, or condensed in the aligned (AC) or staggered (SC) commensurate states. Pair correlation functions for two H_2, at coverages of (a) c =0% and (b) c =67 % of a full monolayer of adsorbed H_2 for a w =8.1 Å pore. The location of peaks in the pair-correlation function of bulk liquid H_2[5] are also marked. Energy per particle as a function of pore width at (c) c =0% and (d) c =67 %. For the thermal distribution, the ground state energy is given. Energy per particle for a w =8.1 Å pore as a function of (e) coverage and (f) condensate fraction in the staggered state.

width w are highly corrugated in the potential energy along the plane, by ∼45 K. As a result, the low-energy single-particle quantum states are heavily perturbed from their free equivalents. These states have peaks in their probability densities which form a triangular lattice with spacing a=2.46 Å. In pores with $w \gtrsim$7 Å, the probability density also separates into two layers at the top and bottom of the pore, as depicted in Figure 1(a).

In considering likely forms for the many-body quantum states, we rely on neutron diffraction experiments [17, 18] which show liquid H_2 on graphene at T = 14-34 K forms an ordered phase commensurate with the underlying lattice, meaning the strong influence of the corrugation persists at high density. The lattice spacing a is smaller than the H_2 hard sphere diameter, d=2.95 Å; below this separation the H_2-H_2 interaction becomes highly repulsive. Thus only every third lattice point is occupied, with an in-plane nearest neighbor distance of a' =4.26 Å. The reciprocal lattice vectors of this triangular H_2 lattice are equal to the wave-vector at the K and K' Dirac points of the underlying graphene lattice. In $w \simeq$7-10 Å pores, the interaction between the top and bottom layers is also significant, and it is important to distinguish whether the two lattices are aligned (Fig. 1(b)) or staggered (Fig. 1(c)).

Matching quantum states may be easily formed from a few single particle states. We used the Mattera *et al.* [16] C-H_2 interaction to find the potential $V_{ext}(\vec{x})$ for a graphene pore, and solved the Schrodinger equation numerically [19] for the H_2 center of mass using periodic boundary conditions for surface area A = 32Å^2. The resultant quantum states are $\psi_{\vec{k},m,n}$, where $\vec{k}$ gives the wavevector parallel to the plane in the first Brioullin Zone, m=1,2... is the band number, and n=0,1... is the quantum number of the confined vibrational motion perpendicular to the plane. Consider the following probability densities,

$$\rho_t = \frac{1}{\sum exp(-\beta E_{\vec{k},m,n})} \sum exp(-\beta E_{\vec{k},m,n}) |\psi_{\vec{k},m,n}|^2 \quad (1)$$

$$\rho_a = |\frac{1}{2}(\psi_{K,1,0} + \psi_{K',1,0}) + \frac{1}{\sqrt{2}}\psi_{0,1,0}|.^2, \quad (2)$$

$$\rho_s = |\frac{1}{2i}(\psi_{K,1,0} - \psi_{K',1,0}) + \frac{1}{\sqrt{2}}\psi_{0,1,1}|.^2, \quad (3)$$

where $\beta = 1/k_bT$. These are the thermally averaged, aligned commensurate (AC), and staggered commensurate (SC) states depicted in Figure 1(a)-(c). Figure 1(d) shows the first two terms of Eq. 3. They describe a real sinusoidal wavefunction whose magnitude alternates between +1, 0, and -1 at adjacent lattice points, which is also in the ground vibrational state. The last term in Eq. 3 is the first excited vibrational state. Because the first two vibrational states (Fig. 1(e)) can be combined to localize the wavefunction at the top or bottom of the pore (Fig. 1(f)), the sum result is to create a wavefunction whose probability density hops between the top and bottom of the pore. The AC state is similarly formed, but without the combination of different vibrational states and thus without the hopping.

As Figure 1 shows, adjacent peaks in the probability density have the largest separation for the SC state. In narrow pores where the distance between the two layers ($l \approx w$-5.8 Å) is small, the SC state is the only one whose adjacent peaks are further apart than d (Fig 2(a)). As a result, the interaction of two H_2 in this state is slightly smaller than for any other pair of states.

When a high density of H_2 is condensed into the SC state, the coherence between the spatial extent of the H_2-H_2 interaction and the natural periodicity of the SC state enhances the latter, futher reducing the interaction

TABLE I. Parameters of the H_2-H_2 interaction functional.

parameter	h	ϵ	σ	c	γ
units	Å	K	Å	K/Å$^{3(1+\gamma)}$	-
value	2.93	34.2	2.96	2.19×10^{10}	4.25

energy for two H_2 in this state.

We calculated the many body quantum states using the mean field approximation, neglecting explicit correlation and exchange effects, and finding system energies $E(N, N_a, N_s)$ and states as a function of number of total particles N, AC particles N_a, and SC particles N_s, with the number of particles thermally distributed $N_t = N - N_a - N_s$. These equations were solved iteratively until self-consistent solutions were found,

$$\rho^{N,N_a,N_s}(\vec{x}) = N_t\rho_t(\vec{x}) + N_a\rho_a(\vec{x}) + N_s\rho_s(\vec{x}) \quad (4)$$

$$V_{dir}^{N,N_a,N_s}(\vec{x}) = \int u[\vec{x},\vec{x}',\rho^{N,N_a,N_s}(\vec{x}')]d\vec{x}', \quad (5)$$

$$\hat{H}^{N,N_a,N_s} = \frac{\hbar^2}{2m}\nabla^2 + V_{ext}(\vec{x}) + V_{dir}^{N,N_a,N_s}(\vec{x}), \quad (6)$$

$$E_{\vec{k},m,n}^{N,N_a,N_s}\ \psi_{\vec{k},m,n}(\vec{x}) = \hat{H}^{N,N_a,N_s}\psi_{\vec{k},m,n}(\vec{x}), \quad (7)$$

$$V_{int}^{N,N_a,N_s} = \int V_{dir}^{N,N_a,N_s}(\vec{x})\rho^{N,N_a,N_s}(\vec{x})d\vec{x}, \quad (8)$$

$$E(N,N_a,N_s) = N_tE_{0,1,0}^{N,N_a,N_s} + N_aE_a^{N,N_a,N_s} + N_sE_s^{N,N_a,N_s} - \frac{1}{2}V_{int}^{N,N_a,N_s}. \quad (9)$$

Small changes in the numerical factors in front of each term in Eqs. 2-3 ensured the probability densities retained the same form. Numerically determined [19] solutions of Eq. 7 are repeated periodically for $A' = 15A$ before use in Eqs. 4-5. Interactions are included through u, a finite-width H_2-H_2 interaction functional,

$$u[\vec{x},\vec{x}',\rho(\vec{x}')] = \rho(\vec{x}')\times\begin{cases}\Phi_{LJ}(|\vec{x}-\vec{x}'|), & |\vec{x}-\vec{x}'|\geq h\\ \Phi_{LJ}(h), & |\vec{x}-\vec{x}'|<h\end{cases} + c\delta(\vec{x}'-\vec{x})\left[\frac{3}{4\pi h^3}\int_{|\vec{x}-\vec{r}|\leq h}\rho(\vec{x}+\vec{r})d\vec{r}\right]^{\gamma}, \quad (10)$$

$$\Phi_{LJ}(r) = 4\epsilon\left[\left(\frac{\sigma}{r}\right)^{12} - \left(\frac{\sigma}{r}\right)^{6}\right], \quad (11)$$

similar to those used for liquid ^{4}He [20, 21]. The second term is increasingly repulsive with density and includes correlation effects in an approximate way. Parameters are given in Table I: ϵ and σ are typical Lennard-Jones parameters,[6] and the remainder reproduce properties of bulk liquid H_2 [21, 22].

We define coverage as $c = 10.7N/(A\times 2)$, where 10.7 Å^2 is the surface area per H_2 at monolayer coverage [17] and the factor 2 accounts for both pore walls. Maximum coverages studied were the ones which hold exactly one H_2 in each peak of the probability density of the SC and AC states, as long as all peaks are at least d apart (resulting in different cutoffs for each state as a function of w, e.g. Fig. 2(e)). Above this density, it is certain that two H_2 are often closer than d and we expect significant correlation effects. The maximum c at any width was $c = 67$ %, equivalent to one commensurate lattice on each side of the pore wall.

The pair correlation function for two particles in the condensate at this maximum coverage is shown in Figure 2(b). It is quite similar to that of bulk liquid H_2.[5] (The major exception is the behavior at $r < 2$ Å; this difference originates from the mean field approximation.) As a result, the interaction of two H_2 in this state is much smaller than for any other pair of states.

Even though the single-particle SC state is always higher in energy than the single-particle ground state (Fig. 2(c)), the tendency of the SC state to reduce the interaction energy means that a condensate in this state becomes the many-body ground state as coverage increases (Fig. 2(d)-(f)) for all pore widths studied. But it is only within a narrower width range, centered around $w \approx 8$ Å, that the energy difference between the SC state and a thermal distribution is large enough (Fig. 2(d)) for a condensate to form at temperatures above the melting point of H_2. It is in this range that the intermolecular interaction and the SC state are closely enough in phase to reduce the interaction energy significantly.

Using the calculated energies $E(N, N_a, N_s)$ and the number of available quantum states,

$$g_t^{N,N_a,N_s}(T) = \sum_{\vec{k},m,n} exp[-\beta(E_{\vec{k},m,n}^{N,N_a,N_s} - E_{0,1,0}^{N,N_a,N_s})], \quad (12)$$

the canonical partition function was computed using Bose statistics, and interpolating between values of N, N_a, N_s. The condensate fraction ($f =< N_s > /N$), average system energy, and specific heat was computed from the partition function. The temperature (through $\beta = 1/k_bT$) was fixed at $T = 20$ K in Eq. 1 and allowed to vary in Eq. 12. As a check, we performed calculations with T variable through the entire calculation for $w = 8.1$ Å, $c = 67\%$, finding over T =20-80 K, only a $\leq$8% variation in the relevant value $E(N_t = N) - E(N_s = N)$.

Figure 3 shows the condensate fraction f, average energy per particle, and specific heat as a function of T for several pore widths at a coverage of $c = 67$ %. There are similarities and differences between this system and a typical BEC. Because condensate formation relies on differences in the interaction energy, there is no simple definition for the critical temperature $T_c(w)$ based on the DOS. Nevertheless, the specific heat (Fig. 3(c)) has the same characteristic cusp as a BEC as f begins to grow, and falls toward the constant of a classical two-dimensional gas at $T > T_c(w)$.

If we define $T_c(w)$ as the location of the cusp, we notice

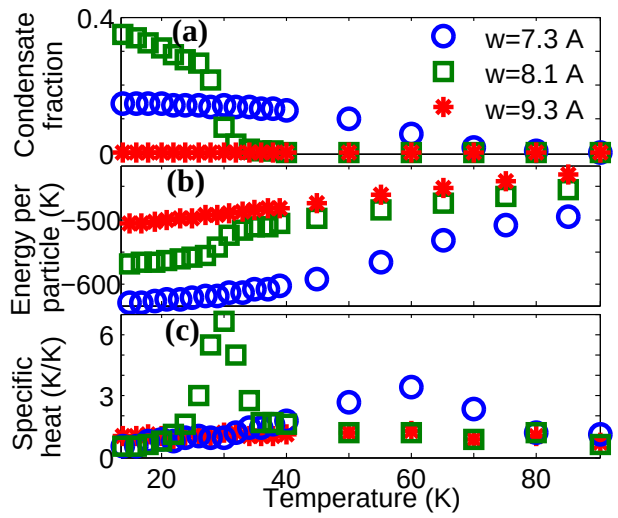

FIG. 3. (a) Condensate fraction, (b) average energy per particle, and (c) specific heat per particle as a function of temperature at 67% coverage for several different pore widths.

$T_c(7.3) = 60$K is much greater than $T_c(8.1) = 30$ K, even though the energy preference for the SC state is larger in an 8.1 Å pore (Fig. 2(d)). This is because the 7.3 Å pore, having a smaller volume, has a smaller number of states g_t. Thus the onset of condensation involves a balance between the areal density of states, g_t/A, which defines the entropic cost of multiple occupation, and the coherence of the SC state with the interparticle interaction, which constrains the energetic benefit of condensation.

While we have not shown $f(c)$, we note that the critical temperature varies less with c (i.e. density) than it may for a typical BEC. Because interactions are an essential part of this new condensate, c must be at least large enough for the interaction energy to become significant enough to make the condensate the many-body ground state, no matter what the temperature.

We also find that the condensate fraction never fully reaches 1. This is because the energy per particle is roughly constant above a certain value of f, as shown in Fig. 2(f). At this critical value (which varies with w), the mean field of the condensate pulls all other states into forms which likewise minimize the interaction energy and there is no longer a significant energetic benefit to increasing f. However, we have not included exchange in our calculations, a factor which tends to favor condensation into a single state [23].

We note that no condensate forms for $w \geq 9.3$ Å. Because the properties of these larger pores approach those of independent graphene sheets, this result is consistent with studies of liquid H_2 on graphene/graphite which have found no evidence of condensation or superfluidity [24] except below the melting temperature in the presence of impurities [25].

Here we have described a unique method of creating a condensate of bosons. While we have presented calculations for a condensate of H_2 which forms in narrow graphene slit-pores, it is likely that other species and/or different pore types may be substituted, as long as the same basic concept is employed: the pore must be designed so that a small subset of quantum states have a periodicity which mimics the high density bulk form, thereby minimizing the interactions and creating a strong energetic preference for those states.

This method has several significant practical advantages when it comes to experimental study of Bose systems. Because formation of a condensate in this system is not singularly dependent on the DOS and thus the temperature, the critical temperatures are orders of magnitude higher than those of other BECs formed of real particles. Not only would this reduce the sophistication and cost of the cooling techniques required, but it also permits higher densities by eliminating the need of super-cooling. Equilibration during cooling and maintenance of the condensate during measurements are simplified both by the higher temperatures and densities allowed, as well as the thermal contact with the underlying structure which provides the trapping potential. However, the optical techniques often used to study BECs will be obscured by the confining pore. Fortunately hydrogen is well suited for scattering studies due to its high neutron cross section, and deep-inelastic scattering has been developed as a technique to study BECs in helium, both in bulk form [26] as well as when adsorbed [27].

While lasers with Å wavelengths have been demonstrated [7], it is likely that formation of the described pore with graphene will be more easily achievable than with an optical lattice. Previous work has demonstrated that graphene slit-pores with controllable widths may be formed from graphene oxide [28] sheets connected by benzene-1,4-diboronic acid linkers, with linker density controlling width. Fortunately, the $w \sim 8$ Å range requires a small density of linkers, and if oxides can be adequately cleaned from the surfaces, this system may represent a likely candidate in which the Bose condensate described here may be observed.

ACKNOWLEDGMENTS

This work was supported by the U.S. Department of Energy Energy Efficiency and Renewable Energy (DOE-EERE) Postdoctoral Research Awards under the EERE Fuel Cell Technologies Program, administered by ORISE for the DOE. ORISE is managed by ORAU (DEAC05-06OR23100). We would like to thank J. Morris, V. Cooper, and G. Vignale for helpful discussions.

* olsenrj@ornl.gov

[1] F. London, Nature **141**, 643 (1938).

[2] M. Anderson, J. Ensher, M. Matthews, C. Wieman, E. Cornell, *et al.*, Science **269**, 198 (1995).

[3] K. B. Davis, M. O. Mewes, M. R. Andrews, N. J. van-Druten, D. S. Durfee, D. M. Kurn, and W. Ketterle, Phys. Rev. Lett. **75**, 3969 (1995).

[4] C. C. Bradley, C. A. Sackett, J. J. TolLett., and R. G. Hulet, Phys. Rev. Lett. **75**, 1687 (1995).

[5] M. Celli, U. Bafile, G. J. Cuello, F. Formisano, E. Guarini, R. Magli, M. Neumann, and M. Zoppi, Phys. Rev. B **71**, 014205 (2005).

[6] Q. Wang and J. Johnson, Mol. Phys. **89**, 1105 (1996).

[7] P. Emma, R. Akre, J. Arthur, R. Bionta, C. Bostedt, J. Bozek, A. Brachmann, P. Bucksbaum, R. Coffee, F.-J. Decker, *et al.*, Nature Photon. **4**, 641 (2010).

[8] J. Kasprzak, M. Richard, S. Kundermann, A. Baas, P. Jeambrun, J. Keeling, M. FM Marchetti, *et al.*, Nature **443**, 409 (2006).

[9] S. Demokritov, V. Demidov, O. Dzyapko, G. Melkov, A. Serga, B. Hillebrands, and A. Slavin, Nature **443**, 430 (2006).

[10] M. R. Matthews, B. P. Anderson, P. C. Haljan, D. S. Hall, C. E. Wieman, and E. A. Cornell, Phys. Rev. Lett. **83**, 2498 (1999).

[11] K. W. Madison, F. Chevy, W. Wohlleben, and J. Dalibard, Phys. Rev. Lett. **84**, 806 (2000).

[12] J. Abo-Shaeer, C. Raman, J. Vogels, and W. Ketterle, Science **292**, 476 (2001).

[13] J. Denschlag, J. Simsarian, D. Feder, C. W. Clark, L. Collins, J. Cubizolles, L. Deng, E. Hagley, K. Helmerson, W. Reinhardt, *et al.*, Science **287**, 97 (2000).

[14] S. Burger, K. Bongs, S. Dettmer, W. Ertmer, K. Sengstock, A. Sanpera, G. V. Shlyapnikov, and M. Lewenstein, Phys. Rev. Lett. **83**, 5198 (1999).

[15] D. S. Jin, J. R. Ensher, M. R. Matthews, C. E. Wieman, and E. A. Cornell, Phys. Rev. Lett. **77**, 420 (1996).

[16] L. Mattera, F. Rosatelli, C. Salvo, F. Tommasini, U. Valbusa, and G. Vidali, Surf. Sci. **93**, 515 (1980).

[17] M. Nielsen, J. McTague, and W. Ellenson, J. Phys. (Paris) **38**, 10 (1977).

[18] M. Nielsen and W. D. Ellenson, in *Proc. 14th Intl. Conf. Low Temp. Phys.*, Vol. 4, edited by M. Krusins and M. Vuorio (1975) p. 437.

[19] S. A. Chin, S. Janecek, and E. Krotscheck, Comput. Phys. Commun. **180**, 1700 (2009).

[20] J. Dupont-Roc, M. Himbert, N. Pavloff, and J. Treiner, J. Low Temp. Phys. **81**, 31 (1990).

[21] E. Krotscheck and J. Navarro, *Microscopic approaches to quantum liquids in confined geometries*, Vol. 4 (World Scientific Publishing Company Incorporated, 2002).

[22] S. Stringari and J. Treiner, Phys. Rev. B **36**, 8369 (1987).

[23] A. J. Leggett, Rev. Mod. Phys. **73**, 307 (2001).

[24] D. M. Ceperley and E. Manousakis, J. Chem. Phys. **115**, 10111 (2001).

[25] M. C. Gordillo and D. M. Ceperley, Phys. Rev. Lett. **79**, 3010 (1997).

[26] S. O. Diallo, J. V. Pearce, R. T. Azuah, O. Kirichek, J. W. Taylor, and H. R. Glyde, Phys. Rev. Lett. **98**, 205301 (2007).

[27] W. Snow and P. E. Sokol, J. Low Temp. Phys. **80**, 197 (1990).

[28] J. W. Burress, S. Gadipelli, J. Ford, J. M. Simmons, W. Zhou, and T. Yildirim, Angew. Chem. Int. Ed. **49**, 8902 (2010).